Preprints.org

Article

Not peer-reviewed version

Bacteriophage St_134 and its Endolysin as a Potential Staphylococcus Biofilm-Removing Biological Agent

Natalia N. Golosova , Andrey L. Matveev * , Nina V. Tikunova , Yana A. Khlusevich , Yulia N. Kozlova , Vera V. Morozova , Igor V. Babkin , Tatiana A. Ushakova , Elena V. Zhirakovskaya , Elisaveta A. Panina , Elena I. Ryabchikova , Artem Y. Tikunov *

Posted Date: 23 January 2024

doi: 10.20944/preprints202312.1650.v2

Keywords: antibiotic resistance; bacteriophage; endolysin; antimicrobial agent; Staphylococcus aureus; Staphylococcus epidermidis; biofilm

Preprints.org is a free multidiscipline platform providing preprint service that is dedicated to making early versions of research outputs permanently available and citable. Preprints posted at Preprints.org appear in Web of Science, Crossref, Google Scholar, Scilit, Europe PMC.

Copyright: This is an open access article distributed under the Creative Commons Attribution License which permits unrestricted use, distribution, and reproduction in any medium, provided the original work is properly cited.

Preprints.org (www.preprints.org) | NOT PEER-REVIEWED | Posted: 23 January 2024 doi:10.20944/preprints202312.1650.v2

Disclaimer/Publisher's Note: The statements, opinions, and data contained in all publications are solely those of the individual author(s) and contributor(s) and not of MDPI and/or the editor(s). MDPI and/or the editor(s) disclaim responsibility for any injury to people or property resulting from any ideas, methods, instructions, or products referred to in the content.

Article

Bacteriophage St_134 and Its Endolysin as a Potential Staphylococcus Biofilm-Removing Biological Agent

Natalia N. Golosova [+], Andrey L. Matveev *[,+], Nina V. Tikunova, Yana A. Khlusevich, Yulia N. Kozlova, Vera V. Morozova, Igor V. Babkin, Tatiana A. Ushakova, Elena V. Zhirakovskaya, Elisaveta A. Panina, Elena I. Ryabchikova and Artem Y. Tikunov *

Institute of Chemical Biology and Fundamental Medicine, Siberian Branch of Russian Academy of Sciences, 630090 Novosibirsk, Russia; n.golosova@g.nsu.ru (N.N.G.); guterus@gmail.com (A.L.M.); tikunova@niboch.nsc.ru (N.V.T.); khlusevichjana@mail.ru (Y.A.K.); ulona@ngs.ru (Y.N.K.); vera_morozova@ngs.ru (V.V.M.); i_babkin@mail.ru (I.V.B.); ushakova@niboch.nsc.ru (T.A.U.); ezhr@niboch.nsc.ru (E.V.Z.); e.panina@g.nsu.ru (E.A.P); lenryab@niboch.nsc.ru (E.I.R.); arttik1986@gmail.com (A.Y.T.)

* Correspondence: guterus@gmail.com, arttik1986@gmail.com

[+] Author with equal contribution

Abstract: Bacteria of the genus *Staphylococcus* are a significant a challenge for medicine, as many species are resistant to multiple antibiotics and even to all of the antibiotics used. One of the approaches to develop new therapeutics to treat staphylococcal infections is the use of bacteriophages specific to these bacteria or lysins of such bacteriophages capable to hydrolyze the cell walls of these bacteria. In this study, a new bacteriophage St_134 specific to *Staphylococcus epedermidis* was described. This small podophage belonging to the Andhravirus genus showed relatively wide host range and was able to infect more than 60 strain of *Staphylococcus spp.*, including a clinical strain from the *Staphylococcus aureus* complex. Two genes encoding different phage lysins were identified in the Ste134 genome. Both lysins LysSte134_1 and LysSte134_2 were produced in *Escherichia coli* cells. Endolysin LysSte134_1 was demonstrated catalytic activity against a wide panel of staphylococcal peptidoglycans (4 species, 6 strains), was active against *S. aureus* and *S. epidermidis* planktonic cultures and destroyed biofilms formed by clinical strains of *S. aureus* and *S. epidermidis*.

Keywords: antibiotic resistance; bacteriophage; endolysin; antimicrobial agent; *Staphylococcus aureus*; *Staphylococcus epidermidis*; biofilm

1. Introduction

In recent decades, the treatment of patients with bacterial infections has often been complicated by the multiple drug resistance (MDR) of causative agents to antibiotics. Among the causative agents, the World Health Organization (WHO) has identified 12 pathogens that pose a global threat to human health [1]. This list includes ESKAPE pathogens and identifies three categories of pathogens depending on their hazard and the urgency of developing new antibacterial drugs. *Staphylococcus aureus* that is resistant to methicillin and vancomycin (MRSA and VRSA) was assigned to the high priority group [2]. Given the faster growth of MDR among nosocomial strains of *Staphylococcus epidermidis* [3] and its increased ability to form biofilms [4–6], an assessment of the antibacterial activity of new drugs against both *S. aureus, S. epidermidis* and other coagulase-negative staphylococci is required.

Among the promising drugs that can become an alternative or addition to antibiotics are bacteriophages. These viruses can specifically infect a bacterial pathogen and eliminate it from the organism. In most cases, phages are safe for the patient's microbiota and after elimination of the target pathogen are excreted naturally without disrupting the functioning of the excretory and immune systems [7–9]. Phages can be used to treat infants, the elderly, and even cancer patients [10–12]. Despite many advantages, the use of bacteriophages has a number of limitations. Only phages with a proven inability to a lysogenic lifestyle and with the absence of undesirable genes in the genome

© 2024 by the author(s). Distributed under a Creative Commons CC BY license.

Preprints.org (www.preprints.org) | NOT PEER-REVIEWED | Posted: 23 January 2024 doi:10.20944/preprints202312.1650.v2

can be used in phage therapy. In addition, the phages used should have high lytic activity and at least two phages that are active against the pathogen should be used to avoid the development of phage resistance [11,13]. Moreover, the usual high specificity of phages requires the selection of personalized phages in each case or the use of phage polyvalent cocktails, which increases the impact on the immune system. Thus, lytic phages with a wide host spectrum and a short, easily annotated genome are preferred for phage therapy.

Phage enzymes capable of destroying bacterial surfaces have advantages over bacteriophages [14–17]. The phage lysins have a wider host spectrum and low bacterial resistance; they demonstrate clear bioavailability and pharmacokinetics [18]. Importantly, standardized biotechnological methods can be used for their production. WHO has recently recognized phage lysins as promising therapeutics [19].

There are three large groups of phage lysins: (1) tail-associated murein lytic enzymes (TAME) that provide genome DNA penetration when the phage adsorbs the host cell; (2) endolysins, which are produced inside the infected cell providing the release of new phage particles; and (3) depolymerases that are able to cleave polysaccharide chains [20–22]. Notably, endolysins can hydrolyze peptidoglycans of the cell wall, being outside. This can be used in particular against gram-positive pathogens and biofilms formed by them. Most phage lysins have a domain structure. Endolysins of phages specific to gram-positive bacteria usually have one or two enzymatically active domains (EAD) and a cell-binding domain (CBD). CBD can be C-terminal or it can be located between two EADs. Many (but not all) endolysins from phages of gram-negative bacteria are small molecules (15 kDa – 20 kDa) and have one EAD or N-terminal CBD plus C-terminal EAD. Based on their lytic activity, all EADs can be divided into five classes: lytic transglycosylases (transferases), which cleave the N-acetylmuramoyl-β-1,4-N-acetylglucosamine bond and four classes of hydrolases, namely 1) N-acetyl-β-D muramidases (lysozymes), endo β-N-acetylglucosaminidases (glucosaminidases), N-acetylmuramoyl-L-alanine amidases, and endopeptidases [23,24]. Notably, the pentaglycine interpeptide bridge is a unique component of most *Staphylococcus* strains that can be digested by the specific peptidoglycan hydrolases [25]. Last years, efficacy of endolysins of phages of Gram-positive bacteria as antibacterial drugs has been demonstrated [18,26–30].

In this study, the *S. epidermidis* phage St_134 was isolated and characterized. This small podophage had the genome of 18,275 bp and was able to infect more than ten coagulase-negative *Staphylococcus* species and one strain from the *Staphylococcus aureus* complex. Two genes encoding different endolysins were found in the St_134 genome and one endolysin was able to destroy peptidoglycans from the cell walls of *S. aureus*, *S. epidermidis*, and *Staphylococcus haemolyticus* as well as their biofilms.

2. Materials and Methods

2.1. Bacterial Strains and Growth Conditions

Escherichia coli strain XL1Blue was used for cloning the lysins genes in the expression plasmid pQE60. Production of the recombinant lysins was carried out in the *E. coli* strain M15. A total of 461 *Staphylococcus* strains (24 species) that were obtained from the Collection of Extremophile Microorganisms and Type Cultures (CEMTC) of ICBFM SB RAS were used to test the host range of the St_134 (Table S1). In addition, *S. aureus* CEMTC 675, *S. aureus* CEMTC 1685, *S. epidermidis* CEMTC 2043, *S. epidermidis* CEMTC 2058, and *S. haemolyticus* CEMTC 3413 were used to investigate the antibacterial activity of lysins Lys-Ste134_1 and LysSte134_2. *Staphylococcus* species was determined by sequencing the 16S rRNA gene fragment (~1400 bp). Antibiotic resistance has been previously tested using the disk-diffusion method (Oxoid™, Thermo Fisher Scientific, Waltham, MA, USA) in accordance with the EUCAST recommendations [3]. All bacterial strains were cultivated in Luria Bertani (LB) media/agar (1.5% w/v) (10 g/L peptone, 5 g/L yeast extract, 10 g/L NaCl, pH: 7.0, Becton Dickinson, Franklin Lakes, NJ, USA). The planktonic bacteria cells were grown in an orbital shaker incubator with 150 rpm at 37°C (Infors HT, Bottmingen, Switzerland).

Preprints.org (www.preprints.org) | NOT PEER-REVIEWED | Posted: 23 January 2024 doi:10.20944/preprints202312.1650.v2

2.2. Phage St_134 Isolation and Propagation

To isolate the phage, 1 mL of sterile phosphate-buffered saline (PBS), pH 7.5 was added to a swab and the obtained suspension was sterilized through a 0.22 μm filter (Wuxi Nest Biotechnology, Wuxi, China). Drops of the filtrate were placed onto freshly prepared lawns of various bacterial cultures in the top agar (Becton, Dickinson and Company Sparks Difco Laboratories, Franklin Lakes, New Jersey, USA). After overnight incubation at 37°C, phage plaques were found on a Petri dish with *S. epidermidis* CEMTC 2058 that was considered the host strain. One plaque was cut from the agar, suspended in sterile PBS, and incubated with shaking overnight to extract phages from the agar. Then, serial ten-fold dilutions were dropped onto a fresh layer of *S. epidermidis* CEMTC 2058 to obtain single plaques. The procedure with a single plaque was repeated four times. Both samples that contained phage and the host strain were collected during the study that was approved by the Ethics Committee of the Novosibirsk Research Institute of Traumatology and Orthopedics (protocol 014/17-2 from 25 November 2011). Both patients whose samples were used to isolate the phage St_134 and its host strain provided informed consents.

To propagate the isolated phage St_134, exponentially growing in LB *S. epidermidis* CEMTC 2058 was infected with St_134 and incubated with shaking at 37°C until the bacterial lysis occurred. The obtained bacterial lysate was clarified by centrifugation at 10,000g for 30 min and phage particles were isolated using precipitation with polyethylene glycol (PEG) 6000 (AppliChem, Darmstadt, Germany) supplemented with NaCl with subsequent centrifugation. Phage precipitate was dissolved in a sterile STM buffer (0.59g of NaCl; 7.88g of Tris-HCl, pH 7.5; and 2.38g of $MgCl_2$ per 1L).

2.3. Electron microscopy

Phage particles were visualized, using transmission electron microscopy (TEM). Formvar-supported copper grid was coated with 10^9 pfu/mL of St_134 phage particles for 1 min. Uranyl acetate was used to contrast the grid with St_134 phage particles. TEM imaging was performed with a TEM JEM 1400 (JEOL, Tokyo, Japan). To obtain digital pictures Veleta digital camera (Olympus SIS, Münster, Germany) was used.

2.4. Biological Properties and Host Range

To evaluate the biological properties of the St_134 phage, *S. epidermidis* CEMTC 2058 was used. All experiments were repeated twice, and each experiment had three replicates. Experiments on phage adsorption rate and burst size were carried out according to [31,32] with minor modifications [33]. To determine the adsorption time, an exponentially growing host cell culture (10^8 CFU/mL) was infected with 10^5 pfu/mL of St_134 (multiplicity of infection, MOI = 0.001). The infected culture was incubated with shaking at 37°C and aliquots were taken every two minutes to determine the titer of free phages by immediate titration. For a one-step growth experiment, 10 mL of exponentially growing host cells were pelleted at 8000g for 10 min and suspended in 500 mkL of LB medium. Phage St_134 was added to the cells with a MOI of 0.001, suspension was incubated for 5 min without shaking at 37°C, and cells were centrifuged. To discard non-adsorbed phage particles, the supernatant was carefully removed and then, the bacterial pellet was resuspended in 10 mL of LB medium. The infected culture was incubated with shaking at 37°C; aliquots were taken and titrated immediately. The lytic activity of the St_134 phage was assessed as described previously [26] with our modifications. Phage St_134 (10^7 pfu/mL) was mixed with *S. epidermidis* CEMTC 2058 culture being in the exponential growth phase with a MOI of 0.1 and incubated without shaking at 37 °C for 30 min to improve infection. Then, infected culture was incubated with shacking and aliquots were taken every 60 min, diluted, seeded on the LB agar and incubated overnight at 37 °C. The bacterial killing curve was evaluated based on counted CFU. To determine the host range for the St_134, phages a spot-assay [34] was carried out using >450 strains belonging to 23 *Staphylococcus* species.

Preprints.org (www.preprints.org) | NOT PEER-REVIEWED | Posted: 23 January 2024 doi:10.20944/preprints202312.1650.v2

2.5. Phage DNA Purification and Complete Genome Sequencing

Genome DNA was isolated from a St_134 stock (10^7 PFU/mL) as described previously [35]. Phage particles were precipitated using a PEG/NaCl solution and suspended in a STM-buffer (10 mM NaCl, 50 mM tris-HCl, pH 8.0, 10 mM MgCl2). The obtained phage suspension was supplemented with 10-25 units DNase I (Thermo Fisher Scientific, Waltham, MA, USA) in DNase I buffer (10 mM tris-HCl pH 7.5, 2.5 mM MgCl2, 0.1 mM CaCl2), up to 10-20 μg/mL RNase (Thermo Scientific), and incubated for 30 min at 37 °C. Then, SDS (final concentration of 0.5%), up to 20 mM of 0.5 M EDTA, pH 8.0, and Proteinase K (up to 100-200 μg/mL) were added followed by incubation at 55 °C for 2-3 hours or at 37 °C overnight. Phage DNA was purified using phenol chloroform extraction with following ethanol precipitation. A paired-end library of phage St_134 DNA was prepared using the NEBNext Ultra II DNA Library Prep Kit for Illumina (New England Biolabs, Inc., Ipswich, MA, USA). Sequencing was carried out using the MiSeq Benchtop Sequencer and MiSeq Reagent Kit v.2 (2 × 250 base reads). The genome was assembled de novo by SPAdes v.3.15.4 and resulted in one genomic contig with an average coverage of 152.

2.6. Comparative Analysis of the Phage St_134 Genome and Proteome

Linearized St_134 genome sequence was imported into online RAST server v. 2.0 [26] to identify the putative ORFs. Functions of the identified ORFs were predicted by BLASTP (NCBI, Bethesda, MD, USA), InterProScan, and HHpred algorithms. Predictions on the architecture of the domains and functional motives were made using CD-BLAST (NCBI, Bethesda, MD, USA). In addition, the results of annotation were manually verified by checking all of the predicted proteins against the NCBI GenBank protein database (https://www.ncbi.nlm.nih.gov, accessed on 19 September 2022).

To compare the St_134 proteome, ViPTree analysis with default parameters [36] was computed by tBLASTx based on genome-wide sequence similarities. ViPTree version 3.7 web server was used (https://www.genome.jp/viptree, accessed on 3 August 23). Phylogenetic analysis of St_134 proteins was performed using Maximum Likelihood. Protein sequences were extracted from the NCBI's protein database using St_134 proteins as query in BLASTp search. Amino acid sequences were aligned using M-Coffee in the T-Coffee program [37]. Phylogenetic trees were constracted by the IQ-tree program v. 2.0.5 [38] the best fit substitution model was applied according to ModelFinder [39]. Branch support was evaluated using 1000 ultrafast bootstrap replicates [40]. All trees were midpoint rooted and visualized in FigTree v1.4.1.

2.7. In Silico Identification and Structural Analysis of Putative Lysins

Lysins LysSte134_1 and LysSte134_2 were predicted using Protein Database from NCBI (https://www.ncbi.nlm.nih.gov/protein, accessed on 15 January 2018) and InterProScan software package (https://www.ebi.ac.uk/interpro, accessed on 15 January 2018). To calculate solubility of LysSte134_1 and LysSte134_2, Protein-sol [41] (https://protein-sol.manchester.ac.uk,) and SoluProt [42] (https://loschmidt.chemi.muni.cz/soluprot) were used. The assumed three-dimensional (3D) structures of the LysSte134_1 and LysSte134_2 lysins were predicted using AlphaFold2 [43] (https://colab.research.google.com/github/sokrypton/ColabFold/blob/main/AlphaFold2.ipynb, accessed on 21–24 April 2023). To visualize ribbon and surface representations of the studied proteins, UCSF Chimera molecular visualizer, version 1.15 [44] was used.

2.8. Cloning, Expression and Purification of Recombinant Lysins

The genes encoding LysSte134_1 and LysSte134_2 lysins were obtained by PCR using Ste134 genomic DNA as a matrix and pairs of primers endolysin_StE134_1U/endolysin_StE134_1L and endolysin_ste134_2u/endolysin_StE134_2L, respectively (Table 1). The expressing plasmid pQE-60 was cleaved using *Nco*I and *Bam*HI (Sibenzyme, Novosibirsk, Russia) and ligated with the obtained PCR fragments that were *Nco*I/*Bam*HI digested too. The obtained plasmids pQE-60/LysSte134_1 and pQE-60/LysSte134_2 were used to transform *E. coli* XL1blue cells. To search *E. coli* clones, containing the corresponding expression plasmids, PCR was performed using primers pQE60-SeqU and

Preprints.org (www.preprints.org) | NOT PEER-REVIEWED | Posted: 23 January 2024 doi:10.20944/preprints202312.1650.v2

pQE60_SeqL (Table 1). Positive clones were sequenced by Sanger sequencing using 3500 Genetic Analyzer (Thermo Fisher Scientific, Waltham, MA, USA).

To optimize the expression of recombinant lysins, *E. coli* M15 cells were transformed with pQE-60/LysSte134_1 or pQE-60/LysSte134_2 plasmids. *E. coli* M15-pQE-60/LysSte134_1 or *E. coli* M15-pQE-60/LysSte134_2 cells were grown on LB-agar with 50 mkg/mL ampicillin at 37°C overnight. To produce recombinant lysins LysSte134_1 and LysSte134_2, fresh colonies of *E. coli* M15-pQE-60/LysSte134_1 or *E. coli* M15-pQE-60/LysSte134_2 were grown in LB medium with 50 mkg/mL ampicillin to reach OD_{600} 0.6-0.7. Then, 0.1 mM isopropyl-β-d-1-thiogalactopyranoside (IPTG) was added and cell cultures were grown overnight with shacking at 150 rpm at 12°C, 20°C, 30°C, and 37°C with shaking at 150 rpm. Then, cells were centrifuged for 10 min at 6000×g, resuspended in 50 mM Tris-HCl pH 8.0, and lysed by sonication using an ultrasonic Sonopuls HD 2070 homogenizer (Bandelin, Mecklenburg-Vorpommern, Germany). Expression level of recombinant proteins and proteins localization was analyzed using polyacrylamide gel (PAAG) with 12.5% SDS.

The recombinant LysSte134_1 protein was purified from the cytoplasm using Ni–NTA Sepharose chromatography (Qiagen, Venlo, Netherlands) according to the manufacturer's instruction. LysSte134_1 was eluted with buffer A (50 mM NaH_2PO_4, 300 mM NaCl, 5 mM Tris-HCl, pH 8.0) containing 100 mM imidazole and concentrated by Amicon Ultra-4 filter (Millipore, Burlington, MA, USA) with a cutoff threshold of 10 kDa. The buffer was replaced with a storage buffer (50 mM Tris-HCl pH 7.5, 300 mM NaCl) by dialysis. Concentration of purified recombinant endolysin was assessed using the Qubit protein assay kit (Thermo Fisher Scientific, Waltham, MA, USA) on a Qubit 4 fluorometer (Thermo Fisher Scientific, Waltham, MA, USA).

Table 1. Primers used for cloning and sequencing.

Primer title	Primer sequence
endolysin_StE134_1U	5`-GGGAACCATGGGAATGAAAAATATTTATTCAAACCACATTAAAGG-3`
endolysin_StE134_1L	5`-GGGATGGATCCGTCAACCTCCAATTTTCCCCAAAGA-3`
endolysin_StE134_2U	5`-CCGAATCATGAATGATAAAGAAAAAATTGACAAGTTTATACAT-3`
endolysin_StE134_2L	5`-CCCAAGGATCCCTTAATACCACTAAAAAACATAATATTATCCCCTG-3`
pQE60-SeqU	5′ - GATTCAATTGTGAGCGGATAAC-3`
pQE60_SeqL	5` - ATCCAGATGGAGTTCTGAGGTC-3`

2.9. Zymography with Peptidoglycans from Staphylococcal Cells

Peptidoglycans from the cell walls of staphylococci were obtained in accordance with the previously described method [45]. A fresh overnight culture of Staphylococcus spp. cells diluted 500 times, and cultured to OD600 = 1-1.5 in 1 L of LB medium at 37 °C, 150 rpm. The cells were centrifuged for 10 min at 6000×g or 8000×g (depending on the *Staphylococcus* species), resuspended in 10 mL of 4 M LiCl, boiled in a water bath for 20 min and re-centrifuged. The precipitate was resuspended in mQ water, disrupted by ultrasonication (35% power) for 25 min using a Sonopuls HD 2070 homogenizer (Bandelin, Berlin, Germany), and centrifuged (12,000×g for 12 minutes). The obtained precipitate was resuspended in 12 mL of 4% SDS, boiled for 20 minutes and pelleted by centrifugation (12 minutes at 12,000×g). The precipitate was resuspended in 12 mL of 1M NaCl and pelleted by centrifugation (12 minutes, 12,000×g). This stage was repeated until the peptidoglycan precipitate became colorless. The resulting peptidoglycan precipitate was suspended in 1-2 mL of mQ water, re-centrifuged, dissolved in 2 mL of mQ water with 0.02% NaN3, and stored at a temperature of 4 °C. The concentration of peptidoglycan was determined using a SmartSpec Plus spectrophotometer (BioRad, Hercules,

Preprints.org (www.preprints.org) | NOT PEER-REVIEWED | Posted: 23 January 2024 doi:10.20944/preprints202312.1650.v2

California, USA). OD_{540} = 1.0 approximately corresponded to the concentration of peptidoglycan 1 mg/mL. To assess the hydrolytic activity, recombinant lysins were fractionated by electrophoresis using SDS-PAAG with purified peptidoglycans at a concentration of 0.1 mg/mL. After electrophoresis, the gel was gently washed with deionized water several times and transferred to a renaturing buffer containing 25 mM Tris–HCl, pH 7.2 and 1% Triton X-100. After incubation at 37°C for 1 hour, the gel was washed several times with deionized water and stained with 1% methylene blue solution.

2.10. Biofilm Assay

To obtained biofilms, staphylococcal cells (2×10^8 CFU) of were resuspended in 200 μL of sterile 0.9% NaCl, mixed with 10 mL of LB medium, and placed in a Petri dish with a pre-sterilized coverslip. The cells were incubated for 5 days at 37°C. On the fifth day, biofilm was evaluated using a Zeiss Axio Imager A2 microscope (Carl Zeiss, Oberkochen, Germany). The formed biofilms were treated with purified endolysin at a concentration of 25 mkg/mL in PBS. PBS without endolysin was used as a negative control. Treated biofilms were incubated at 37°C and stained with 0.1% methyl violet.

2.11. Statistical Analyses

The statistical analysis was carried out by one-way analysis of variance (ANOVA) using Statistica 10 software (StatSoft. Inc., USA). The differences between the groups were considered significant at $p < 0.05$.

3. Results

3.1. St_134 Isolation, Plaques and Phage Particles Morphology

Phage St_134 was found in a skin wash sample that was obtained from a patient with psoriasis. The clinical strain *S. epidermidis* CEMTC 2058 that was used as a bacterial host has been previously isolated from a purulent wound and kindly provided by our colleagues from the Novosibirsk Research Institute of Traumatology and Orthopedics. Its taxonomy was confirmed by sequencing of the 16S rRNA gene (GenBank ID OP393915). On the fresh lawn of the host strain, the phage St_134 formed cloudy plaques with a diameter of 0.8–1 mm.

Electron microscopy indicated that St_134 is a relatively small podophage with icosahedral head (Ø 37–40 60 nm) connected to a short non-contractile tail (Figure 1).

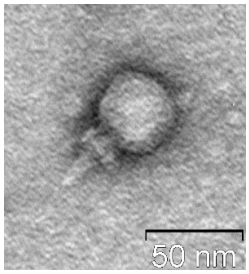

Figure 1. Electron micrograph of St_134 phage particle negatively stained with 1% uranyl acetate.

3.2. St_134 Biological Properties and Host Range

To characterize biological properties of the phage St_134, the host strain *S. epidermidis* CEMTC 2058 was used. Absorption experiment indicated that approximately 85% of St_134 phage particles attached to host cells within 22 min (Figure 2A). One step growth assay showed that the latent period for St_134 was ~45 min and a burst size was ~12 phage particles per infected cell (Figure 2B). The multistep bacterial killing experiments revealed that phage was not highly virulent (Figure 2C).

Preprints.org (www.preprints.org) | NOT PEER-REVIEWED | Posted: 23 January 2024 doi:10.20944/preprints202312.1650.v2

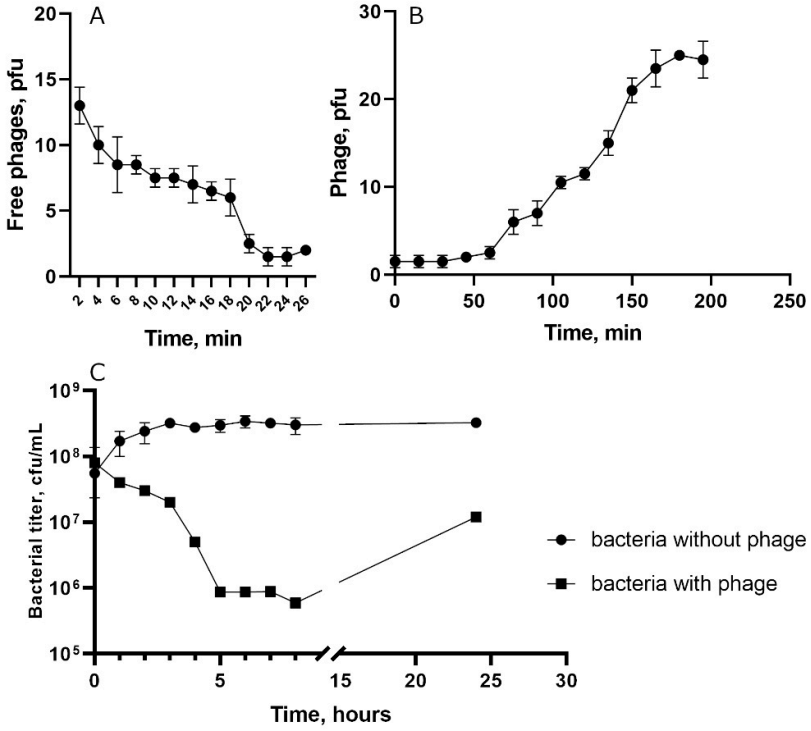

Figure 2. Biological properties of the phage St 134: (A) phage adsorption to host cells; (B) burst size experiments; (C) bacterial lytic curve.

To determine the phage host range, 461 *Staphylococcus* strains of 23 various species were used (Table 2). Of them, 446 strains were obtained from clinical samples and 15 strains were obtained from pets. Among tested strains, 204 were coagulase-positive *S. aureus* and *S. intermedius*; however, only one strain (*S. roterodami*/*S. argenteus* CEMTC 3692) was susceptible to St_134 infection. Other 357 strains were coagulase-negative *Staphylococcus*, and 61 strains from them were St_134-sensitive, including six strains obtained from pets. (CEMTC number, resistance to antibiotics, and GenBank ID of all St_134-sensitive staphylococcal strains are presented in Table S1). Most of the susceptible strains were *S. epidermidis* and both antibiotic-sensitive and antibiotic-resistant (or even MDR) strains were identified among St_134-susceptible ones. Other 24 strains that were sensitive to St_134 included: three *S. haemolyticus* strains with MDR; all tested *S. capitis*, *S. caprae*, *S. casei*, *S. cohnii*, and *S. lugdunensis* (all of them were antibiotic-sensitive); and single strains from other species, some of which were antibiotic-resistant or even MDR (Table 2, Table S1).

Table 2. *Staphylococcus* strains tested for their sensitivity to the St_134 phage.

№	Species	Number of tested strains	Number of strains sensitive to St_134
	Coagulase-positive *Staphylococcus* spp.		
1	*S. aureus*	178	0
2	*S. aureus* complex *(S. roterodami/S. argenteus)*	1	1
3	*S. intermedius*	25	0
	Coagulase-negative *Staphylococcus* spp.		
4	*S. epidermidis*	136	37 (27.2%)
5	*S. auricularis*	5	1
6	*S. borealis*	2	0
7	*S. capitis*	4	4
8	*S. caprae*	5	5

Preprints.org (www.preprints.org) | NOT PEER-REVIEWED | Posted: 23 January 2024 doi:10.20944/preprints202312.1650.v2

9	*S. carnosus*	2	0
10	*S. casei*	2	2
11	*S. coagulans*	8	1
12	*S. cohnii*	5	2
13	*S. devriesei*	4	1
14	*S. equorum*	4	2
15	*S. felis*	6	0
16	*S. haemolyticus*	28	3 (10.7%)
17	*S. hominis*	22	0
18	*S. lugdunensis*	2	2
19	*S. pasteuri*	1	0
20	*S. saprophyticus*	2	0
21	*S. simulans*	8	0
22	*S. succinus*	1	0
23	*S. ureilyticus*	1	1
24	*S. warneri*	9	0
	Total	**461**	**62**

3.3. St_134 Genome Characteristics and Comparative Analysis

The St_134 genome is double-stranded linear DNA of 18,275 bp. Twenty putative ORFs were found and nine of them are oriented in the forward direction, whereas eleven ORFs are in opposite direction (Figure 3). Among 20 ORFs, 17 ORFs encode proteins with predicted functions (Table S2) and only three ORFs encode hypothetical proteins. The first block of ORFs contains the genes encoding the DNA polymerase, terminaze large subunit, several virion proteins, including virion-associated tail tip lysin, and three relatively small hypothetical proteins. The second block consists of genes encoding the holing, endolysin, and structural proteins (Figure 3).

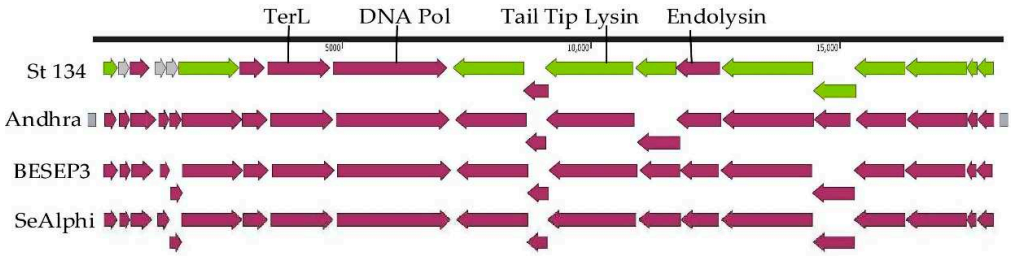

Figure 3. Genome maps of the St_134 phage and *Staphylococcus* phages from the *Andhravirus* genus. Terminal repeats of the genome of the phage Andhra are marked with gray squares. ORFs encoding structural and hypothetical proteins are marked with green and grey, respectively.

Comparative genome analysis indicated that the St_134 phage is a member of the *Andhravirus* genus (*Rountreeviridae* family). The genomes of all known phages from the *Andhravirus* genus are similar in size (~18 kb) and their organization is similar too. All genomes contain 20 ORFs divided into the same two blocks according to the ORFs orientation (Figure 3). Most genes are orthologous and located in the same positions in the genomes of the *Andhravirus* species. ViPTree analysis confirmed taxonomy of St_134 (Figure 4). Notably, all members of the *Andhravirus* genus and neighbor *Rosenblumvirus* genus infect *Staphylococcus* spp.

Preprints.org (www.preprints.org) | NOT PEER-REVIEWED | Posted: 23 January 2024 doi:10.20944/preprints202312.1650.v2

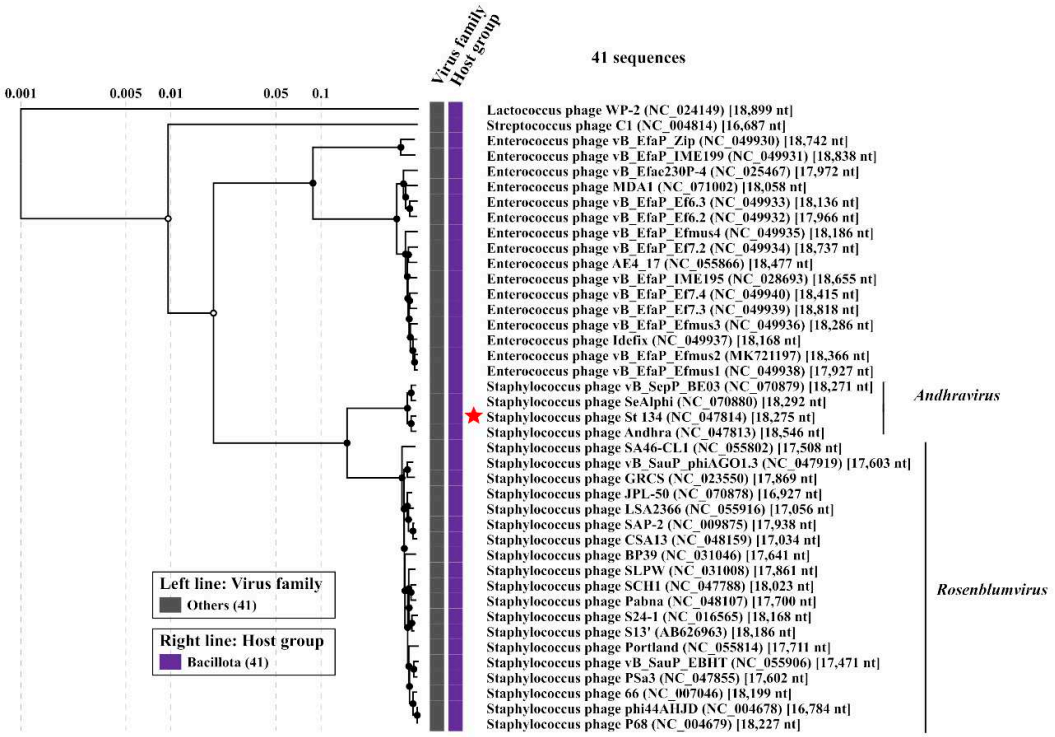

Figure 4. ViPTree analysis of the *Staphylococcus* phage St 134 that is marked with a red asterisk.

3.3. Phylogenetic analysis of the St_134 Proteins

Phylogenetic analysis was performed for the St_134 terminaze large subunit, tail tip lysin, and endolisin (Figure 5). In each case, 40 most similar sequences according to the BLASTp comparison were used for analysis. On the Maximum Likelihood (ML) phylogenetic tree of the St 134 terminate large subunit, phage sequences of the *Andhravirus* genus form a monophyletic, highly supported clade (Figure 5). Several unknown phage sequences from the metagenome assembled genomes (MAGs) are grouped with this clade. The remaining sequences belong to the *Rosenblumvirus* genus and are clustered separately (Figure 5A).

The topology of the ML tree containing the St_134 tail tip lysin is similar (Figure 5B). Analysis of the St_134 tail tip lysin using BLASTp demonstrated that it has 89% similarity (100% coverage) with the Andhra phage protein gp10 (tail tip lysin gp10, YP_009789375.1). This lysin contains N-terminal glycosyl hydrolase (GyH) domain and C-terminal cysteine-histidine-dependent amidohydrolases/peptidases (CHAP) domain. A clade of sequences of the genus *Andhravirus* is also formed with high reliability and divided into two subclades. The remaining sequences belong to the genus *Rosenblumvirus* and are grouped separately. As for the endolysin phylogeny, only four sequences from the known *Andhraviruses*, including the St_134 and Andhra phages, are found on the ML tree. St_134 endolysin (LysSte134_1) sequence showed 81% similarity (100% coverage) with the Andhra phage protein gp14 (N-acetylmuramuramoyl-L-alanine amidase, YP_009789379). Three additional sequences from MAGs are grouped with them. The remaining sequences have a low level of similarity with endolysin sequences from the *Andhravirus* genus (Figure 5C).

Preprints.org (www.preprints.org) | NOT PEER-REVIEWED | Posted: 23 January 2024 doi:10.20944/preprints202312.1650.v2

A

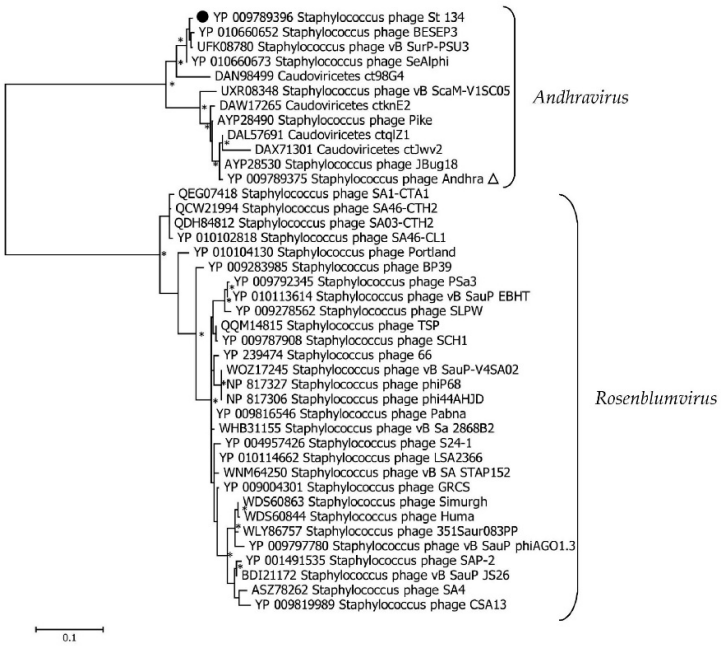

B

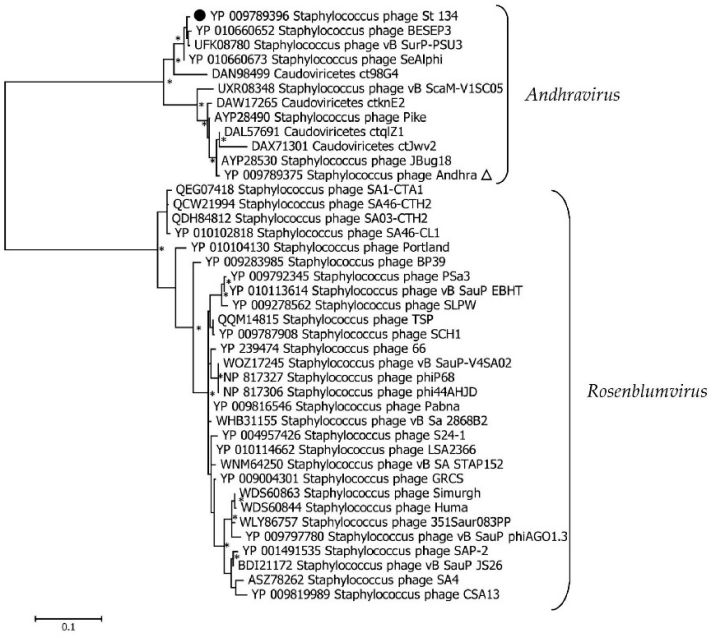

C

Preprints.org (www.preprints.org) | NOT PEER-REVIEWED | Posted: 23 January 2024 doi:10.20944/preprints202312.1650.v2

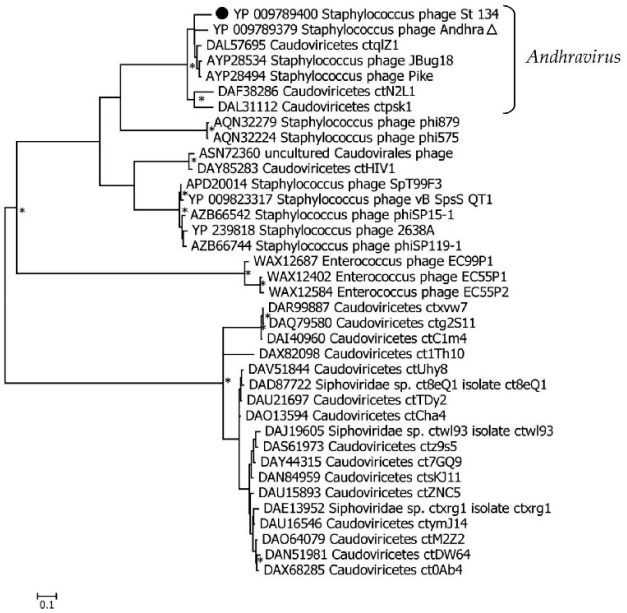

Figure 5. Maximum Likelihood phylogenetic trees of the St_134 terminase large subunit (A), tail tip lysin (B), and endolysin (C) generated using IQ-tree software. Corresponding sequences of the St_134 phage are marked with black circles; sequences of *Staphylococcus* phage Andhra are marked with triangles. Nodes with 95% statistical significance calculated from 1000 ultrafast bootstrap replicates are marked with asterisks. The scale bar represents the number of substitutions per site.

3.3. In Silico Characterization of St_134 lysins

The putative endolysin LysSte134_1 consists of 295 amino acids (aa) with an isoelectric point (pI) of 9.21 and a predicted molecular weight of 35 kDa. InterPro software package (https://www.ebi.ac.uk/interpro/search/sequence/, accessed 21.08.2023) was used to determine the LysSte134_1 domains. It was shown that LysSte134_1 belongs to the superfamily of N-acetylmuramoyl-L-alanine amidase/peptidoglycan recognition proteins (Amidase/PGRP_sf) (IPR036505) and contains two domains. The N-terminal domain is the N-acetylmuramoyl-L-alanine amidase-like type II (NALAA-2, EC 3.5.1.28, EC 3.5.1.28) domain (IPR002502). In the LysSte134_1 sequence, the NALAA-2-like catalytic domain (pfam01510) is located between 22 and 147 aa residues. The C-terminal region (190-295 aa) of LysSte134_1 has similarity with SH3 domains (G3DSA:2.30.30.40).

The putative structure of LysSte134_1 was predicted using AlphaFold2. It was confirmed that Lys Ste134_1 consists of two domains. The N-terminal globular core contains the predicted enzymatic NALAA-2-like domain that connects to the C-terminal globular SH3 domain via an unordered linker (Figure 6). The N-terminal NAALA-2-like domain contains four α-helices and one β-sheet; the C-terminal domain consists of two β-sheets interlinked by flexible linkers. Ligand-binding site of LysSte134_1 was predicted using meta-server approach to protein-ligand binding site prediction COFACTOR. It was predicted that the catalytic zinc ion (Zn^{2+}) is coordinated with His27, His135, and Cys143 (Figure 6).

The putative tail tip lysin LysSte134_2 contains 472 aa with pI of 8.91 and predicted molecular weight of 51.4 kDa. HHpred, InterPro (https://www.ebi.ac.uk/interpro/search/sequence/, accessed 21.08.2023), and CDD database were used to identify the domain structure. It was indicated that LysSte134_2 belongs to the superfamily NLPC_P60 and contains two enzymatic domains: N-terminal GyH and C-terminal CHAP endopeptidase (IPR007921). The C-terminal domain is similar to CATH-Gene3D 3DSA:3.90.1720.10. The N-terminal GyH-like domain is located between 10 and 183 aa resides, whereas CHAP domain (Pfam PF05257) is located between 351 and 439 aa residues. The cysteine, histidine-dependent amidohydrolases/peptidases (CHAP) hydrolyze peptidoglycans in the bacterial cell wall.

Preprints.org (www.preprints.org) | NOT PEER-REVIEWED | Posted: 23 January 2024 doi:10.20944/preprints202312.1650.v2

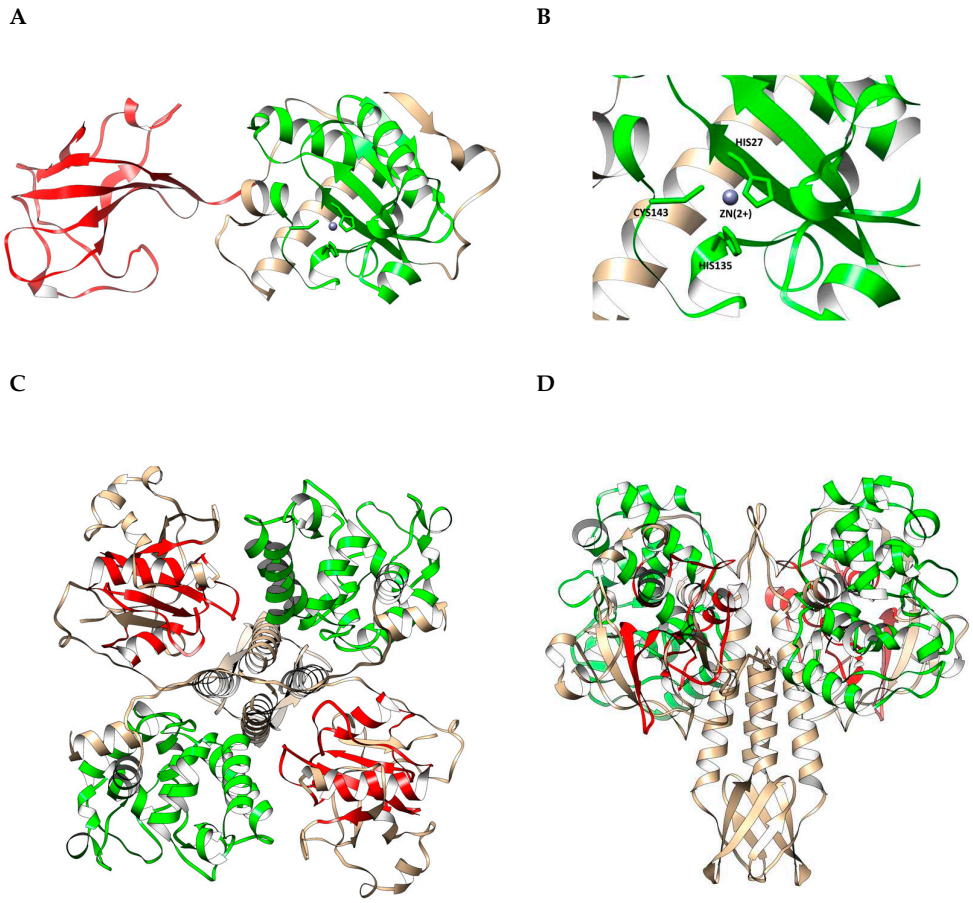

Figure 6. (A) Ribbon representation of the predicted 3D structure of the endolysin LysSte134_1 in complex with Zn2+ ion; EAD and SH3 are marked in red and green, respectively. (B) Ribbon representation of the putative zinc-binding site of LysSte134_1; His27, His135, and Cys143) are shown in a stick representation. (C) Ribbon representation (top view) of the predicted 3D dimer structure of the lysin LysSte134_2; GyH and CHAP are marked in green and red, respectively. (D) Ribbon representation (side view) of the predicted 3D dimer structure of the lysin LysSte134_2; GyH and CHAP are marked in green and red, respectively. The molecular coordinates of the predicted 3D structure of St_134 lysins were rendered using UCSF Chimera molecular visualizer, version 1.15.

AlphaFold2 showed that the putative 3D structure of LysSte134_2 is similar to the Andhra gp10 protein [46]. In LysSte134_2, the N-terminal globular core contains the predicted enzymatic GyH-like domain and connects to the C-terminal globular CHAP domain via an ordered linker domain (middle linker). This linker domain consists of two α-helices and one β-sheet (Figure 6). Probably, LysSte134_2 form homodimer like gp10 of the Andhra phage (Figure 6). The N-terminal GyH-like domain contains eight α-helices; the C-terminal CHAP-like domain consists of two α-helices and one β-sheet.

Solubility of putative recombinant LysSte134_1 and LysSte134_2 was assessed using SoluProt and Protein-sol bioinformatics tools. SoluProt demonstrated that both putative lysins have suitable solubility scores (> 0.5) to be produced in *E. coli* cells. However, analysis using Protein-sol indicated that while LysSte134_1 has solubility scores adequate (~ 0.45), LysSte134_2 has solubility scores insufficient for production in *E. coli* cells (much less than 0.45).

Preprints.org (www.preprints.org) | NOT PEER-REVIEWED | Posted: 23 January 2024 doi:10.20944/preprints202312.1650.v2

3.4. Cloning, Production and Purification of LysSte134_1 and LysSte134_2

The genes encoding the lysins LysSte134_1 and LysSte134_2 were inserted into the expression plasmid pQE-60. To produce the recombinant the lysins LysSte134_1 and LysSte134_2 the constructed plasmids pQE-60-LysSte134_1 and pQE-60-LysSte134_2 were used to transform *E. coli* M15 cells. Various growth conditions were tested to increase solubility of the recombinant lysins. The localization and yield of LysSte134_1 and LysSte134_2 were evaluated using PAAG electrophoresis (Figure S1). LysSte134_1 was found in the soluble fraction of the cytoplasm only after cultivation of *E. coli* M15/pQE-60-LysSte134_1 cells at 10°C and induction with 100 μM IPTG. LysSte134_1 was purified using Ni-NTA agarose from a soluble fraction of cytoplasm and its molecular weight was ~35 kDa, which corresponded to the predicted one (Figure 7). The purity of LysSte134_1 after chromatography was evaluated using PAGE and it was ~95% (Figure 7). The yield of LysSte134_1 production was 2 mg from 1 L of cell culture after all stages of purification and dialysis. The purified LysSte134_1 was stored at a concentration of more than 1 mg/ml in buffer S (50 mM Tris-HCl pH 7.5, 300 mM NaCl) at 4°C.

Unlike LysSte134_1, the recombinant LysSte134_2 was insoluble under any cultivation conditions. Several attempts were made to refold LysSte134_2 from the insoluble cytoplasm fraction as described previously [47]. During dialysis, LysSte134_2 precipitated when the concentration of urea in the re-coagulation buffer was below 1 M. So, a purified soluble preparation of this protein was not obtained and the insoluble fraction of the cytoplasm was used to assess the enzymatic activity of the protein.

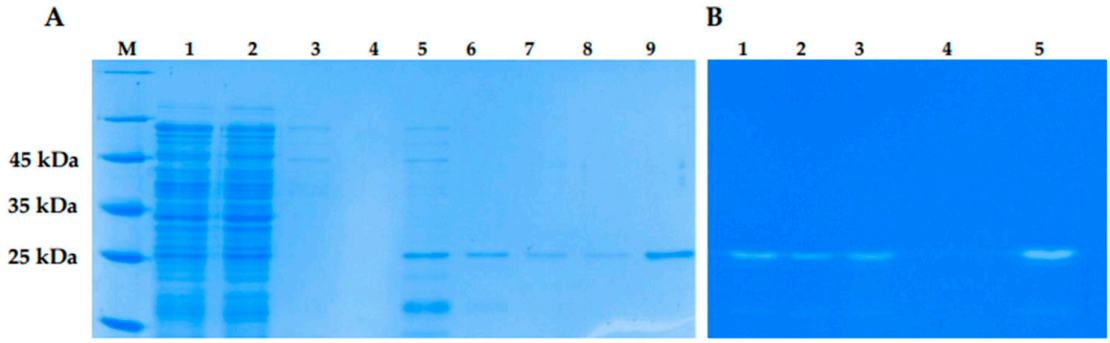

Figure 7. SDS PAAG electrophoreses (A): 1 - lysates of *E. coli* M15-pQE-60/LysSte134_1 cells producing recombinant LysSte134_1; 2 – soluble cytoplasm of *E. coli* M15- pQE-60/LysSte134_1; 3 – eluate from Ni-NTA agarose after washing with buffer A (50 mM NaH2PO4, pH 8.0, 300 mM NaCl, 5 mM Tris-HCl); 4 – 9 - eluate from Ni-NTA agarose after elution with buffer A, containing 50 mM, 100 mM, 150 mM, 200 mM, 250 mM and 350 mM imidazole, correspondingly. (B) Zymographic assay of eluate from Ni-NTA agarose after elution with buffer A, containing 100 mM (1); 150 mM (2) ; 200 mM (3), 250 mM (4) and 350 mM (5) M- protein ladder Precision Plus Protein™ Standards (Bio-Rad, Hercules, CA, USA). PAGE (12,5%) containing 0.5 mg of peptidoglycan from *S. epidermidis* CEMTC 2058.

3.5. Enzymatic activity of LysSte134_1 and LysSte134_2

The lytic activity of LysSte134_1 and LysSte134_2 lysins was assessed by zymographic assay using cell wall peptidoglycans of various *Staphylococcus* strains as substrates. It was shown that LysSte134_1 hydrolyzed peptidoglycan from the cell wall of *S. epidermidis* CEMTC 2058 that is a host strain of St_134 phage (Figure 7). In addition, LysSte134_1 was able to digest peptidoglycans from other coagulase-negative strains, namely *S. epidermidis* CEMTC 2043 (insensitive to St_134 strain with MDR), *S. haemolyticus* CEMTC 3413 (MDR), and *S. warneri* CEMTC 2062 (weak activity) (Figure 8). However, it could not cleave peptidoglycans isolated from the cell wall of *S. warneri* CEMTC 4154 and both tested *S. saprophyticus* strains CEMTC 3872 and CEMTC 6829. Notably, the parental St_134 phage did not infect all tested *S. warneri* and *S. saprophyticus* strains (Table 2, Table S1).

Preprints.org (www.preprints.org) | NOT PEER-REVIEWED | Posted: 23 January 2024 doi:10.20944/preprints202312.1650.v2

It is worth noting that LysSte134_1 hydrolyzed peptidoglycans from the cell wall of the coagulase-positive strains *S. aureus* CEMTC 675 and *S. aureus* CEMTC 1685 (Figure 8). *S. aureus* CEMTC 675 is resistant to cefoxitin, gentamicin, erythromycin, and clindamycin (strain with MDR), whereas *S. aureus* CEMTC 1685 is resistant to lincomycin and vancomycin (VRSA) and both *S. aureus* strains are not susceptible to St_134 infection. The obtain results demonstrated that LysSte134_1 is able to hydrolyze peptidoglycan from various pathogenic the cell wall of the *Staphylococcus* strains despite their resistance to antibiotics and sensitivity to the parental phage St_134 (Figure 8). LysSte134_2 did not hydrolyze any of the investigated peptidoglycans isolated from various *Staphylococcus* cells walls.

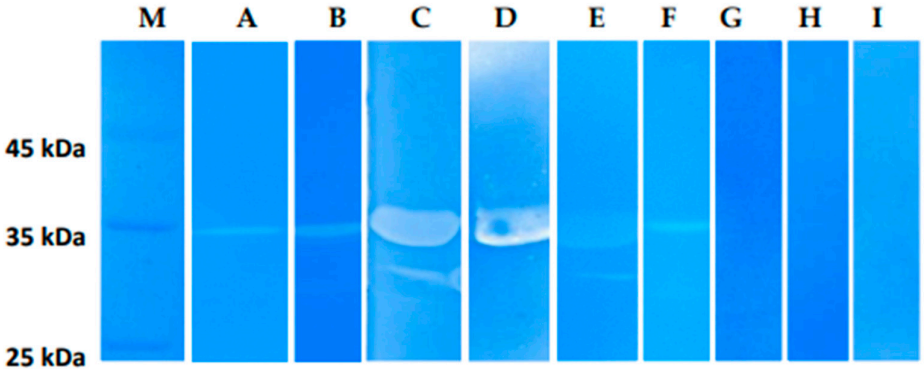

Figure 8. Zymographic analysis of recombinant LysSte134_1. PAGE (12,5%) containing 0.5 mg of peptidoglycan from *S. aureus* CEMTC 675 (A), *S. aureus* CEMTC 1685 (B), *S. epidermidis* CEMTC 2058 (C), *S. epidermidis* CEMTC 2043 (C), *S. haemolyticus* CEMTC 3753 (E), *S. warneri* CEMTC 2062 (F), *S. warneri* CEMTC 4154 (G), *S. saprophyticus* CEMTC 3872 (H), *S. saprophyticus* CEMTC 6829 (H), stained with methylene blue. M - protein ladder Precision Plus Protein™ Standards (Bio-Rad, Hercules, CA, USA).

3.6. Anti-Staphylococcal Activity of LysSte134_1

The antibacterial activity of LysSte134_1 was assessed against a planktonic culture *S. aureus* CEMTC 1685 and *S. epidermidis* CEMTC 2058. It was demonstrated that treatment of *S. aureus* CEMTC 1685 or *S. epidermidis* strain CEMTC 2058 cells with LysSte134_1 (25 μg/ml) resulted in a 50-fold decrease in CFU (Figure 9). Then, the effect of different concentrations of bivalent ions (Ca^{2+}, Mg^{2+}, Zn^{2+}, and Ni^{2+}) on effectivity of LysSte134_1 was studied. When *S. aureus* CEMTC 1685 and *S. epidermidis* CEMTC 2058 were treated with LysSte134_1 that was supplemented with $ZnCl_2$ at concentrations of 1 μM and 5 μM, lytic activity of LysSte134_1 against these strains increased up to 100-fold and 1000-fold, respectively (Figure 9). Notably, Ca^{2+}, Mg^{2+}, and Ni^{2+} did not significantly affect the hydrolytic activity of LysSte134_1 against both tested S*taphylococcus* strains.

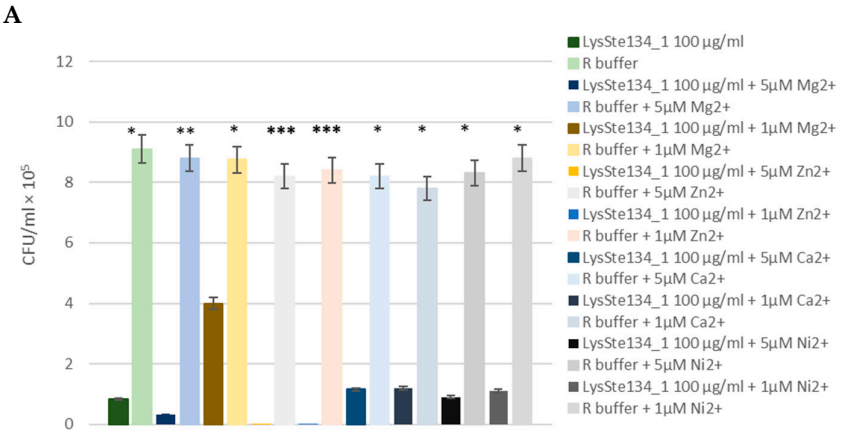

Preprints.org (www.preprints.org) | NOT PEER-REVIEWED | Posted: 23 January 2024 doi:10.20944/preprints202312.1650.v2

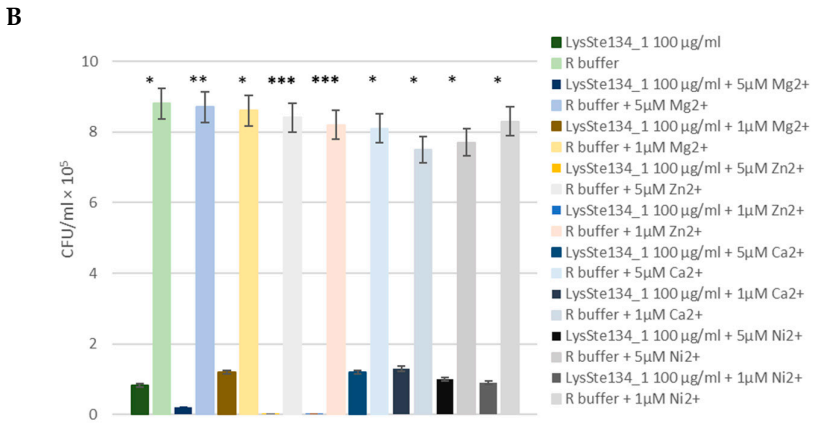

Figure 9. Antibacterial activity of LysSte134_1 against S. aureus CEMTC 1685 (A) and S. epidermidis CEMTC 2043. LysSte134_1 (100 µg/ml) was added to staphylococcal cells with or without $CaCl_2$, $MgSO_4$, $ZnCl_2$, or $NiSO_4$ and the obtained suspensions were incubated for two hours before viable colonies counting. Cell cultures with only $CaCl_2$, $MgSO_4$, $ZnCl_2$, or $NiSO_4$ were used as controls. Experiments were performed in triplicate. *** $p < 0.001$, ** $p < 0.01$, * $p < 0.05$.

3.7. Biofilm Disruption Activity of LysSte134_1

LysSte134_1 activity against staphylococcal biofilms was evaluated using biofilms formed by *S. epidermidis* CEMTC 2043 and *S. aureus* CEMTC 1685. Both strains are insensitive to St_134 infection and *S. epidermidis* CEMTC 2043 is resistant to cefixime, erythromycin, ciprofloxacin/levofloxacin, chloramphenicol, and vancomycin, whereas *S. aureus* CEMTC 1685 is a VRSA strain. Biofilms were grown on the surface of coverslips in LB medium. When biofilms were formed, they were treated with purified LysSte134_1 at a concentration of 25 µg/mL in PBS. Sterile PBS was added as a control. Biofilms with LysSte134_1 were incubated at 37°C for 30 min and 120 min, while biofilms with PBS were incubated for ~180 minutes. In *S. epidermidis* biofilm treated with LysSte134_1, only small remains of biofilm matrix and cells were observed after incubation for 30 min (Figure 10). LysSte134_1 was not so active against biofilm formed by *S. aureus* cells; however, even this biofilm was sustantualy disrupted within 30 min. In control biofilms, a tight matrix of stained bacteria was observed (Figure 10)

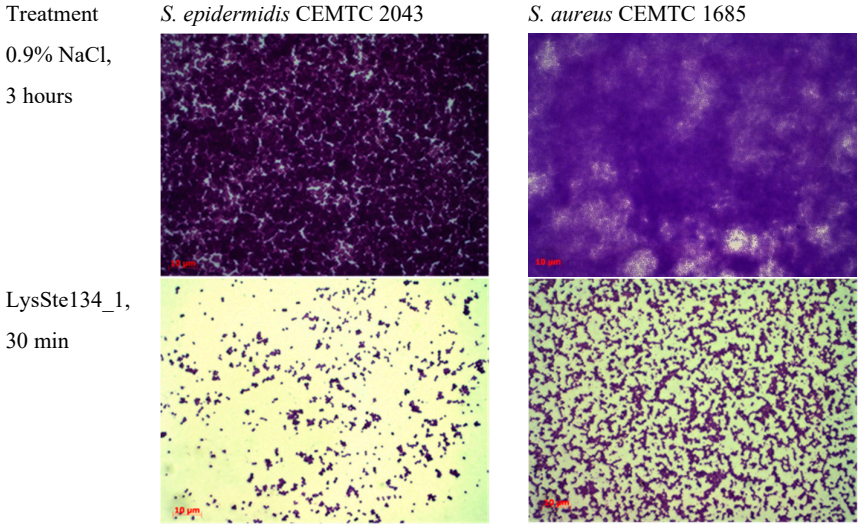

Preprints.org (www.preprints.org) | NOT PEER-REVIEWED | Posted: 23 January 2024 doi:10.20944/preprints202312.1650.v2

LysSte134_1, 120 min

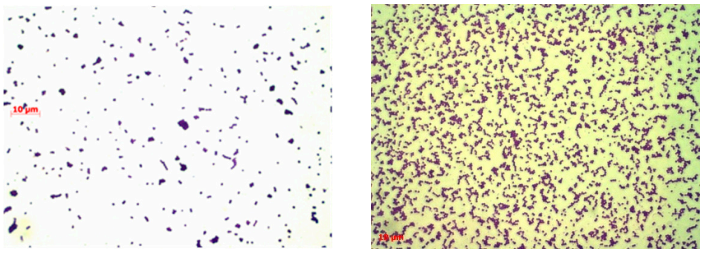

Figure 10. LysSte134_1 activity against biofilms that were formed by *S. epidermidis* CEMTC 2043 and *S. aureus* CEMTC 1685. Bacterial cells were stained with methylene blue.

4. Discussion

Phage-encoded lysins are promising agents against drug-resistant bacterial pathogens. In this study, the functional and in silico structural analysis of recombinant lysins LysSte134_1 and LysSte134_2 was performed. The genes encoding these lysins were cloned using the genome of the lytic *Staphylococcus epidermidis* phage St_134. This small podophage is a typical member of the *Andhravirus* genus (*Rountreeviridae* family). Like its close relatives, namely *Staphylococcus* phages Andhra [46,48], BESEP3 (GenBank: MT596500.1), and SeAlphi (NCBI: NC_070880.1), the bacterial host of St_134 is *S. epidermidis*. Several other coagulase-negative *Staphylococcus* species were sensitive to St_134, including *S. haemolyticus*. However, we did not find *S. saprophyticus* and *S. warneri* strains that can be infected with St_134 as well as coagulase-positive *S. aureus* and *S. intermidius* strains, despite the fact that >200 strains were tested. Nevertheless, one coagulase-positive strain (CEMTC 3692) was found to be susceptible to St_134 infection. It was a member of the *S. aureus* complex. Sequencing of its 16S rRNA gene fragment (1364 bp) indicated high nucleotide identity (NI) with *Staphylococcus roterodami* (NI = 100%) and *Staphylococcus argenteus* (NI = 99.93%). These two species are part of the *S. aureus* complex and were isolated from a human foot infection and hip joint infection [49,50]. So, we can conclude that the phage St_134 has a relatively wide host range.

The genes encoding both types of lysins were found in the St_134 genome: Lys-Ste134_1 that is produced in the host cell cytoplasm providing the release of new phage particles (endolysin) and LysSte134_2, which cleaves the cell walls peptidoglycans after phage adsorption (tail-associated lysin). Endolysin LysSte134_1 belongs to the N-acetylmuramoyl-L-alanine amidase/peptidoglycan recognition proteins (Ami-dase/PGRP_sf) superfamily. It contains N-terminal NALAA-2-like catalytic domain and C-terminal SH3 domain. Usually, amidases from the NALAA-2 group are Zn2+-dependent enzymes that cleaved the amide linkage between N-acetylmuramoyl and L-amino acids in the bacterial cell wall [51]. In the endolysin LysSte134_1, Zn2+ presumably bound with His28, His130, and Cys138. The tail-associated lysin LysSte134_2 consists of the N-terminal GyH-like domain connected to the C-terminal CHAP domain via linker domain (structured linker), that formed dimer structure of LysSte134_2.

Despite the fact that solubility of LysSte134_1 was predicted as acceptable for production in *E. coli* cells, this protein was produced in a soluble form only when *E. coli* culture was grown at 10°C. Unfortunately, our attempts to obtain enzimaticaly active LysSte134_2 were unsuccessful. Zymographic assay, using peptidoglycans from various *Staphylococcus* cells revealed that LysSte134_1 hydrolyzed peptidoglycans from both coagulase-positive (*S. aureus*) and coagulase-negative (*S. epidermidis*, *S. haemolyticus*, and one *S. warneri*) *Staphylococcus* spp. In addition, LysSte134_1 showed antibacterial activity against both *S. aureus* and *S. epidermidis*. Moreover, the ability of LysSte134_1 to disrupt biofilms formed by *S. aureus* and *S. epidermidis* was confirmed.

Phylogenetic analysis indicated that the most similar lysins to the studied LysSte134_1 and LysSte134_2 are well-characterized lysins of the Andhra phage [46,48]: Andhra_gp10, which that is a homologue of LysSte134_2 and Andhra_gp14 that is a homologue of LysSte134_1. It was shown that Andhra_gp1 had moderate hydrolytic activity and Andhra_gp10 demonstrated strong hydrolytic activity against peptidoglycans *in vitro.* In the growth inhibition test, both gp10 and gp14 proteins suppressed the growth of *S. epidermidis* and *Staphylococcus intermedius* strains, with little or no effect

Preprints.org (www.preprints.org) | NOT PEER-REVIEWED | Posted: 23 January 2024 doi:10.20944/preprints202312.1650.v2

on the growth rate of *S. aureus* [46]. Such differences are probably due to the fact that although Andhra_gp14 and LysSte134_1 are similar proteins, their similarity rate is only 80%. The largest number of substitutions in both endolysins is located in the NALAA-2 and SH3 domains, which probably leads to an increase in the spectrum of lytic activity of LysSte134_1. Unfortunately, the hydrolytic activity of LysSte134_1 against peptidoglycans from *S. intermedius* and planctonic culture was not tested, which is a limitation of this study. It should be done in future.

Both *S. aureus* and *S. intermedius* are coagulase-positive staphylococci; however, they belong to different complexes. Usualy, strains from the *S. aureus* complex can cause various severe infections in humans including meningitis and sepsis, whereas strains from the *S. intermedius* complex are mainly causative agents of veterinary infections and can be transmitted to humans through contacts with animals [52–54]. High lytic activity of LysSte134_1 against planktonic cultures of *S. aureus* and biofilms that were formed by *S. aureus* is an advantage of the LysSte134_1 endolysin. Notably, LysSte134_1 showed even higher efficacy against *S. epidermidis* cells and biophilms that against *S. aureus* ones. Although it is believed that *S. epidermidis* is a less virulent pathogen than *S. aureus*, in recent years the proportion of *S. epidermidis* strains with MDR is significantly higher than that for *S. aureus* at least in some regions [3]. In addition, *S. epidermidis*, being a normal skin commensal, is capable of forming biofilms, which is a serious problem in intensive care units and especially in surgery.

In conclusion, taking into consideration hydrolytic activity of LysSte134_1 against both coagulase-positive *S. aureus* and coagulase-negative *Staphylococcus* spp., we can consider this endolysin as a promising antibacterial agent that is able to remove staphylococcal biofilms. In addition, such phage lysins can be used in combination with antibiotics, as they can digest and destroy the biofilm matrix, which facilitates antibiotics to reach the target cells and, in turn, can lead to a decrease in the dosage of antibiotics.

Supplementary Materials: The following supporting information can be downloaded at the website of this paper posted on Preprints.org. Table S1. *Staphylococcus* spp. strains sensitive to the St_134 phage. Table S2. Open reading frames (ORFs) found in the genome of the St_134 phage. Figure S1:-SDS PAAG electrophoreses (A): 1 - lysates of *E. coli* M15-pQE-60/LysSte134_1 cells, producing recombinant LysSte134_1; 2 – insoluble cytoplasm of *E. coli* M15- pQE-60/LysSte134_1; 3 –soluble cytoplasm of *E. coli* M15- pQE-60/LysSte134_1. (B): 1 - lysates of *E. coli* M15-pQE-60/LysSte134_2 cells, producing recombinant LysSte134_2; 2 – insoluble cytoplasm of *E. coli* M15- pQE-60/LysSte134_1; 3 – soluble cytoplasm of *E. coli* M15- pQE-60/LysSte134_2.

Author Contributions: Conceptualization, A.L.M. and N.V.T.; methodology V.V.M., A.L.M. and Y.N.K.; validation, N.N.G., I.V.B., Y.A.K., A.L.M., and E.A.P.; data curation, N.N.G., V.V.M., and A.L.M.; formal analysis, N.N.G., A.L.M., V.V.M., E.A.P., E.V.Z. and Y.A.K.; funding acquisition, A.Y.T.; investigation, T.A.U., N.N.G., E.I.R., Y.N.K., E.A.P., E.V.Z., A.L.M., and A.Y.T.; visualization, N.N.G., Y.N.K., E.I.R., T.A.U., I.V.B., and A.L.M.; writing—original draft, Y.A.K. A.L.M., and N.V.T.; writing—review and editing, Y.A.K., N.V.T., and A.Y.T.; supervision, N.V.T. All authors have read and agreed to the published version of the manuscript.

Funding: This work was supported by the Russian state-funded project for ICBFM SB RAS (grant number 122110700002-2).

Institutional Review Board Statement: Samples that contained phage and the host strain were collected during the study that was approved by the Ethics Committee of the Novosibirsk Research Institute of Traumatology and Orthopedics (protocol 014/17-2 from 25 November 2011).

Informed Consent Statement: Both patients whose samples were used to isolate the phage St_134 and its host strain provided informed consents.

Data Availability Statement: Not applicable.

Acknowledgments: The authors would like to thank their colleagues from the Novosibirsk Research Institute of Traumatology and Orthopedics the strain and clinical sample provided.

Conflicts of Interest: The authors declare no conflict of interest. The funder had no role in the design of the study, in the collection, analysis, and interpretation of data, in writing the manuscript, or in the decision to publish the results.

Preprints.org (www.preprints.org) | NOT PEER-REVIEWED | Posted: 23 January 2024 doi:10.20944/preprints202312.1650.v2

References

1. De Oliveira, D.M.P.; Forde, B.M.; Kidd, T.J.; Harris, P.N.A.; Schembri, M.A.; Beatson, S.A.; Walker, M.J. Antimicrobial Resistance in ESKAPE Pathogens. *Clinical Microbiology Reviews*, **2020**, *33(3)*, e00181-19.
2. Tacconelli, E.; Carrara, E.; Savoldi, A.; Harbarth, S.; Mendelson, M.; Monnet, D.L., Carmeli, Y. Discovery, research, and development of new antibiotics: the WHO priority list of antibiotic-resistant bacteria and tuberculosis. *The Lancet Infectious Diseases*, **2018**, *18(3)*, 318–327
3. Bardasheva, A.; Tikunov, A.; Kozlova, Y.; Zhirakovskaia, E.; Fedorets, V.; Fomenko, N.; Kalymbetova, T.; Chretien, S.; Pavlov, V.; Tikunova, N.; Morozova, V. Antibiotic Resistance and Pathogenomics of Staphylococci Circulating in Novosibirsk, Russia. *Microorganisms* **2021**, *9*(12), 2487.
4. Becker, K.; Heilmann, C.; Peters, G. Coagulase-Negative Staphylococci. *Clinical Microbiology Reviews* **2014**, *27*(4), 870–926.
5. Otto, M. Staphylococcus epidermidis Pathogenesis. *Methods Mol Biol* **2014**, *1106*, 17–31.
6. Paharik, A.E.; Horswill, A.R. The Staphylococcal Biofilm: Adhesins, Regulation, and Host Response. *Virulence Mechanisms of Bacterial Pathogens* **2016**, *50*, 529–566.
7. Morozova, V.V.; Vlassov, V.V.; Tikunova, N.V. Applications of Bacteriophages in the Treatment of Localized Infections in Humans. *Frontiers in Microbiology* **2018**, *9*, 1696. doi:10.3389/fmicb.2018.01696
8. Petrovic Fabijan, A.P; Lin, R.C.Y.; Ho, J.; Maddocks, S.; Ben Zakour, N.L.; Iredell, R. Safety of bacteriophage therapy in severe Staphylococcus aureus infection. *Nat Microbiol* **2020,** *5(3)*, 465–472. doi:10.1038/s41564-019-0634-z
9. Kaźmierczak, Z.; Majewska, J.; Milczarek, M.; Owczarek, B.; Dąbrowska, K. Circulation of Fluorescently Labelled Phage in a Murine Model. *Viruses*. **2021**;*13(20),* 297. doi:10.3390/v1302029
10. Chanishvili, N. Bacteriophages as Therapeutic and Prophylactic Means: Summary of the Soviet and Post-Soviet Experiences. *Curr Drug Deliv* **2016,** *13*, 309–323.
11. Schooley, R.T.; Biswas, B.; Gill, J.J.; Hernandez-Morales, A.; Lancaster, J.; Lessor, L.; Barret J.J. Development and Use of Personalized Bacteriophage-Based Therapeutic Cocktails To Treat a Patient with a Disseminated Resistant Acinetobacter baumannii Infection [published correction appears in Antimicrob Agents Chemother. *Antimicrob Agents Chemother*. **2017**; *61(10),* e00954-17. doi:10.1128/AAC.00954-17
12. Chan, B.K.; Turner, P.E.; Kim, S.; Mojibian, H.R.; Elefteriades, J.A.; Narayan, D. Phage treatment of an aortic graft infected with *Pseudomonas aeruginosa*. *Evol Med Public Health*. **2018,** *2018(1)*, 60–66. doi:10.1093/emph/eoy005
13. Morozova, V.; Kozlova, Y.; Ganichev, D.; Tikunova, N. Bacteriophage Treatment of Infected Diabetic Foot Ulcers. In: Methods in Molecular Biology, Joana Azeredo and Sanna Sillankorva (Eds): Bacteriophage Therapy, **2018**, *1693*, 151–158. DOI 10.1007/978-1-4939-7395-8
14. Schmelcher, M.; Donovan, D.M.; Loessner, M.J. Bacteriophage endolysins as novel antimicrobials. *Future Microbiol* **2012**, *7*(10), 1147–1171.
15. Gondil, V.S.; Harjai, K.; Chhibber, S. Endolysins as Emerging Alternative Therapeutic Agents to Counter Drug-Resistant Infections. *Int. J. Antimicrob. Agents* **2020**, *55*, 105844.
16. Abdelrahman, F.; Easwaran, M.; Daramola, O.; Ragab, S.; Lynch, S.; Oduselu,T.J.; Khan, F.M.; Ayobami, A.; Adnan, F.; Torrents, E.; Sanmukh, S.; El-Shibiny1, A. Phage-Encoded Endolysins *Antibiotics (Basel)* **2021**, *10*(2), 124.
17. Murray, E.; Draper, L.A.; Ross, R.P.; Hill, C. The Advantages and Challenges of Using Endolysins in a Clinical Setting. *Viruses* **2021**, *13*, 680
18. Harhala, M.A.; Gembara, K.; Nelson, D.C.; Miernikiewicz, P.; Dabrowska, K. Immunogenicity of Endolysin PlyC. *Antibiotics* **2022**, *11*, 966. https://doi.org/10.3390/antibiotics11070966
19. WHO. *2020 Antibacterial Agents in Clinical and Preclinical Development*; World Health Organization: Geneva, Switzerland, 2021; 76p.
20. Adhya, S.; Merril, C.R.; Biswas, B. Therapeutic and Prophylactic Applications of Bacteriophage Components in Modern Medicine. *Cold Spring Harb. Perspect. Med.* **2014**, *4*, a012518
21. São-José, C. Engineering of Phage-Derived Lytic Enzymes: Improving Their Potential as Antimicrobials. *Antibiotics* **2018**, *7*, 29.
22. Latka, A.; Maciejewska, B.; Majkowska-Skrobek, G.; Briers, Y.; Drulis-Kawa, Z. Bacteriophage-Encoded Virion-Associated Enzymes to Overcome the Carbohydrate Barriers during the Infection Process. *Appl. Microbiol. Biotechnol.* **2017**, *101*, 3103–3119.
23. Rodríguez-Rubio, L.; Gerstmans, H.; Thorpe, S.; Mesnage, S.; Lavigne, R.; Briers, Y. DUF3380 Domain from a Salmonella Phage Endolysin Shows Potent N -Acetylmuramidase Activity. *Appl. Environ. Microbiol.* **2016**, *82*, 4975–4981.
24. Höltje, J.V.; Mirelman, D.; Sharon, N.; Schwarz, U. Novel Type of Murein Transglycosylase in Escherichia Coli. *J. Bacteriol.* **1975**, *124*, 1067–1076.
25. Rajagopal, M.; Walker, S. Envelope Structures of Gram-Positive Bacteria. *Curr Top Microbiol Immunol*. **2017**, *404*, 1–44.

Preprints.org (www.preprints.org) | NOT PEER-REVIEWED | Posted: 23 January 2024 doi:10.20944/preprints202312.1650.v2

26. Gilmer, D. B.; Schmitz, J. E.; Thandar, M.; Euler, C.W.; Fischetti, V.A. The Phage Lysin PlySs2 Decolonizes Streptococcus suis from Murine Intranasal Mucosa. *PloS one* **2017**, *12*(1), e0169180. https://doi.org/10.1371/journal.pone.0169180
27. Gutiérrez, D., Garrido, V., Fernández, L., Portilla, S., Rodríguez, A., Grilló, M. J., García, P. Phage Lytic Protein LysRODI Prevents Staphylococcal Mastitis in Mice. *Frontiers in microbiology* **2020**, *11*, 7. https://doi.org/10.3389/fmicb.2020.00007
28. Miernikiewicz, P.; Barylski, J.; Wilczak, A.; Dragoš, A.; Rybicka, I.; Bałdysz, S.; Szymczak, A.; Dogsa, I.; Rokush, K.; Harhala, M.A.; Ciekot, J.; Ferenc, S.; Gnus, J.; Witkiewics, W.; Dabrowska, K. New Phage-Derived Antibacterial Enzyme PolaR Targeting Rothia spp. *Cells* **2023**, *12*, 1997. https://doi.org/10.3390/cells12151997
29. Kim, H.; Seo, J. A Novel Strategy to Identify Endolysins with Lytic Activity against Methicillin-Resistant Staphylococcus aureus. *Int. J. Mol. Sci.* **2023**, *24*, 5772. https://doi.org/10.3390/ijms24065772
30. Li, X.; Wang, S.; Nyaruaba, R.; Liu, H.; Yang, H.; Wei, H.A. Highly Active Chimeric Lysin with a Calcium-Enhanced Bactericidal Activity against *Staphylococcus aureus* In Vitro and In Vivo. Antibiotics (Basel). **2021**, *19*, 461. doi: 10.3390/antibiotics10040461
31. Pajunen, M.; Kiljunen, S.; Skurnik, M. Bacteriophage phiYeO3-12, specific for Yersinia enterocolitica serotype O:3, is related to coliphages T3 and T7, *J Bacteriol*, **2000**, *182*, 5114–5120. doi:10.1128/JB.182.18.5114-5120.2000
32. Kropinski, A.M. Measurement of the rate of attachment of bacteriophage to cells. In: *Bacteriophages: methods and protocols*, Clokie M.R.J., Kropinski, A.M.; Humana Press; New York, USA, 2009; pp. 151-155. doi:10.1007/978-1-60327-164-6_15
33. Morozova, V.; Kozlova, Y.; Jdeed, G.; Tikunov, A.; Ushakova, T.; Bardasheva, A.; Zhirakovskaia, E.; Poletaeva, Y.; Ryabchikova, E.; Tikunova, N. A Novel Aeromonas popoffii Phage AerP_220 Proposed to Be a Member of a New Tolavirus Genus in the Autographiviridae Family. *Viruses* **2022**, *14*, 2733. doi: 10.3390/v14122733
34. Kutter, E. Phage host range and efficiency of plating. In: *Bacteriophages: methods and protocols*, Clokie M.R.J., Kropinski, A.M.; Humana Press; New York, USA, **2009**; Volume 1, pp. 141–149. doi:10.1007/978-1-60327-164-6_14
35. O'Flaherty, S.; Coffey, A.; Edwards, R.; Meaney, W.; Fitzgerald, G.F.; Ross, R.P. Genome of staphylococcal phage K: a new lineage of Myoviridae infecting gram-positive bacteria with a low GC content. *J Bacteriol* **2004**, *186*, 2862–2871.
36. Nishimura, Y.; Yoshida, T.; Kuronishi, M.; Uehara, H.; Ogata, H.; Goto, S. Viptree: The viral proteomic tree server. *Bioinformatics* **2017**, *33*, 2379–2380. https://doi.org/10.1093/bioinformatics/btx157
37. Notredame, C.; Higgins, D.G.; Heringa, J. T-Coffee: A novel method for fast and accurate multiple sequence alignment. *J. Mol. Biol.* **2000**, *302*, 205–217. https://doi.org/10.1006/jmbi.2000.4042
38. Nguyen, L.T.; Schmidt, H.A.; von Haeseler, A.; Minh, B.Q. IQ-TREE: A Fast and Effective Stochastic Algorithm for Estimating Maximum-Likelihood Phylogenies. *Mol. Biol. Evol.* **2015**, *32*, 268–274. https://doi.org/10.1093/molbev/msu300
39. Kalyaanamoorthy, S.; Minh, B.Q.; Wong, T.K.F.; von Haeseler, A.; Jermiin, L.S. ModelFinder: Fast Model Selection for Accurate Phylogenetic Estimates. *Nat. Methods* **2017**, *14*, 587–589. https://doi.org/10.1038/nmeth.4285
40. Minh, B.Q.; Nguyen, M.A.T.; von Haeseler, A. Ultrafast Approximation for Phylogenetic Bootstrap. *Mol. Biol. Evol.* **2013**, *30*, 1188–1195. https://doi.org/10.1093/molbev/mst024
41. Hebditch, M.; Carballo-Amador, M.A.; Charonis, S.; Curtis, R.; Warwicker, J. Protein–Sol: A web tool for predicting protein solubility from sequence. *Bioinformatics* **2017**, *33*, 3098–3100.
42. Hon, J.; Marusiak, M.; Martinek, T.; Kunka, A.; Zendulka, J.; Bednar, D.; Damborsky, J. SoluProt: Prediction of soluble protein expression in Escherichia coli. *Bioinformatics* **2021**, *37*, 23–28.
43. Mirdita, M.; Schutze, K.; Moriwaki, Y.; Heo, L.; Ovchinnikov, S.; Steinegger, M. Colab-Fold: Making protein folding accessible to all. *Nat. Methods* **2022**, *19*, 679–682.
44. Pettersen, E.F.; Goddard, T.D.; Huang, C.C.; Couch, G.S.; Greenblatt, D.M.; Meng, E.C.; Ferrin, T.E. UCSF Chimera—a visualization system for exploratory research and analysis. *J. Comput. Chem.* **2004**, *25(13)*, 1605–1612. https://doi.org/10.1002/jcc.20084
45. Fukushima, T.; Sekiguchi, J. Zymographic Techniques for the Analysis of Bacterial Cell Wall in Bacillus. *Methods Mol Biol*. **2016**, *1440*, 87-98.
46. Hawkins, N. C., Kizziah, J. L., Hatoum-Aslan, A., Dokland, T. Structure and host specificity of Staphylococcus epidermidis bacteriophage Andhra. *Science advances*, **2022**, *8(48)*, eade0459. https://doi.org/10.1126/sciadv.ade0459
47. Matveev,A., Khlusevich, Y., Golota, O., Kravchuk, B., Tkachev, S., Emelyanova, L., Tikunova, N. Tick-borne encephalitis nonstructural protein NS1 expressed in E. coli retains immunological properties of the native protein. *Protein expression and purification*, **2022**, *191*, 106031. https://doi.org/10.1016/j.pep.2021.106031

Preprints.org (www.preprints.org) | NOT PEER-REVIEWED | Posted: 23 January 2024 doi:10.20944/preprints202312.1650.v2

48. Cater, K., Dandu, V. S., Bari, S. M., Lackey, K., Everett, G. F., Hatoum-Aslan, A. A Novel Staphylococcus Podophage Encodes a Unique Lysin with Unusual Modular Design. *mSphere*, **2017**, *2(2),* e00040-17. https://doi.org/10.1128/mSphere.00040-17
49. Schutte, A. H. J., Strepis, N., Zandijk, W. H. A., Bexkens, M. L., Bode, L. G. M., Klaassen, C. H. W. Characterization of Staphylococcus roterodami sp. nov., a new species within the Staphylococcus aureus complex isolated from a human foot infection. *International journal of systematic and evolutionary microbiology* **2021**, *71(9)*. https://doi.org/10.1099/ijsem.0.004996
50. Tong, S. Y. C., Schaumburg, F., Ellington, M. J., Corander, J., Pichon, B., Leendertz, F., Bentley, S. D., Parkhill, J., Holt, D. C., Peters, G., Giffard, P. M. Novel staphylococcal species that form part of a Staphylococcus aureus-related complex: the non-pigmented Staphylococcus argenteus sp. nov. and the non-human primate-associated Staphylococcus schweitzeri sp. nov. *International journal of systematic and evolutionary microbiology*, **2015**, *65(Pt 1)*, 15–22. https://doi.org/10.1099/ijs.0.062752-0
51. Vermassen, A.; Leroy, S.; Talon, R.; Provot, C.; Popowska, M.; Desvaux, M. Cell Wall Hydrolases in Bacteria: Insight on the Diversity of Cell Wall Amidases, Glycosidases and Peptidases Toward Peptidoglycan. *Front. Microbiol*. **2019**, *10*, 331.
52. Somayaji, R.; Priyantha, M.A.; Rubin, J.E.; Church, D. Human infections due to Staphylococcus pseudintermedius, an emerging zoonosis of canine origin: report of 24 cases. *Diagn Microbiol Infect Dis*. **2016**, *85*, 471–476. doi:10.1016/j.diagmicrobio.2016.05.008
53. Darlow, C.A.; Paidakakos, N.; Sikander, M.; Atkins, B. A spinal infection with Staphylococcus pseudintermedius. *BMJ Case Rep.* **2017**, *2017,* bcr2017221260. doi:10.1136/bcr-2017-221260
54. Magleby, R.; Bemis, D.A.; Kim, D.; Carroll, K.C.; Castanheira, M.; Kania, S.A.; Jenkins, S.G.; Westblade, L.F. First reported human isolation of Staphylococcus delphini. *Diagn Microbiol Infect Dis*. **2019**, *94*, 274–276. doi:10.1016/j.diagmicrobio.2019.01.014

Disclaimer/Publisher's Note: The statements, opinions and data contained in all publications are solely those of the individual author(s) and contributor(s) and not of MDPI and/or the editor(s). MDPI and/or the editor(s) disclaim responsibility for any injury to people or property resulting from any ideas, methods, instructions or products referred to in the content.